Time-Resolved Small-Angle Neutron Scattering Study of Spinodal Decomposition in Deuterated and Protonated Polybutadiene Blends

ARTICLE *in* THE JOURNAL OF CHEMICAL PHYSICS · SEPTEMBER 1993

Impact Factor: 2.95 · DOI: 10.1063/1.466225

4 AUTHORS, INCLUDING:

Hiroshi Jinnai
Tohoku University
234 PUBLICATIONS **4,217** CITATIONS
SEE PROFILE

Hirokazu Hasegawa
Kyoto University
163 PUBLICATIONS **4,887** CITATIONS
SEE PROFILE

Takeji Hashimoto
Kyoto University
516 PUBLICATIONS **16,947** CITATIONS
SEE PROFILE

Time-resolved small-angle neutron scattering study of spinodal decomposition in deuterated and protonated polybutadiene blends. I. Effect of initial thermal fluctuations

Hiroshi Jinnai, Hirokazu Hasegawa, and Takeji Hashimoto
Department of Polymer Chemistry, Kyoto University, Kyoto 606-01 Japan

Charles C. Han
Polymers Division, National Institute of Standards and Technology, Gaithersburg, Maryland 20899

(Received 26 March 1993; accepted 17 June 1993)

Time-resolved small-angle neutron scattering (SANS) experiments have been performed on the self-assembling process of a binary mixture of deuterated polybutadiene and protonated polybutadiene at the critical composition. This mixture has an upper critical solution temperature type of phase diagram with the spinodal temperature at 99.2 °C. Specimens held in the single-phase state at an initial temperature (T_i) were quenched to a point inside the spinodal phase boundary at a final temperature (T_f) to induce phase separation via spinodal decomposition (SD). In order to examine the effect that thermal concentration fluctuations have on SD, three different initial temperatures, T_i=102.3 °C, 123.9 °C, and 171.6 °C, were chosen while T_f was fixed at −7.5 °C. The time-dependent SANS structure factor, $S(q,t;T_f)$, showed clear scattering peaks corresponding to the early and intermediate stages of SD. The time changes in the wave number $q_m(t;T_f)$ and the intensity $S_m(t;T_f)$ at the peak of $S(q,t;T_f)$ followed different paths depending on the initial temperature. This fact evidences a definite effect of thermal concentration fluctuations on SD (i.e., a significant "memory" effect). A critical test of the linearized Cahn–Hilliard–Cook theory led to the conclusion that this theory can describe satisfactorily the early stage SD in the deep-quench region.

I. INTRODUCTION

Studies of miscibility and phase separation kinetics of polymer blends are of current interest from both industrial and academic points of view. From the former view point, they provide information useful in developing new materials with better properties by controlling the miscibility and phase-separated structures of polymer blends. From the academic view point, such studies of self-assembling processes, patterns (morphology), and dynamics via spinodal decomposition (SD) provide challenging research themes related to nonequilibrium nonlinear phenomena of long-chain molecules through experiments,[1,2] theories,[3–16] and computer simulations[6–9] studies.

Over the past decade, a number of experimental studies[10–13] have been made on the coarsening kinetics of phase-separated structure of polymer mixtures. The results have shown that the coarsening process of a polymer mixture with a critical composition can be classified into, at least, the following three stages: (i) early stage; (ii) intermediate stage; and (iii) late stage.[11]

In the early stage of SD, the time evolution of concentration fluctuations is well described by the linearized theory first formulated by Cahn for small molecule systems.[14] It predicts (i) the wave number $q_m(t;T)$ is independent of time t, where $q_m(t;T)$ corresponds to the peak position of the structure factor at t and at the phase separating temperature T; (ii) the amplitude of concentration fluctuation $\Delta\phi(\mathbf{q},t)$ with wave vector $\mathbf{q}$ grows exponentially with t. Prediction (i) assumes that the system is quenched from the single-phase state in which thermal concentration fluctuations are sufficiently small. The definition of the wave vector $\mathbf{q}$ is given below in Sec. II. Many reports have confirmed that in the early stage of SD, $\Delta\phi(\mathbf{q},t)$ grows exponentially with t, but, in the intermediate stage of SD, the time evolution of concentration fluctuations becomes increasingly nonlinear in nature[6] and the phase-separated structure coarsens with time, giving rise to a nonexponenital variation of $\Delta\phi(\mathbf{r},t)$ and a decrease in $q_m(t;T)$ with t. In the late stage of SD,[11] a well-defined interface is developed between two coexisting domains and the amplitude of spatial concentration fluctuation $\Delta\phi(\mathbf{r},t)$ reaches an equilibrium value $\Delta\phi_e$,[15] where $\mathbf{r}$ is the position vector. In this stage, the sizes of the domains still grow and hence $q_m(t;T)$ further decreases thereby to reduce the excess free energy associated with the interface area.[16]

There are two basic problems that remain unclear in regard to the early stage SD. Problem 1 is concerned with how the wave number $q_m(t;T)$ at the maximum of scattering intensity changes with time in this stage. No data adequate for this problem are as yet available because the light scattering (LS) method commonly used so far for SD studies has no power to explore the region of high q where the maxima are expected to appear in the very beginning of SD.

Problem 2 is whether the Cahn–Hilliard–Cook (CHC)[17] theory is capable of predicting accurately the early stage SD, especially the time dependence of $q_m(t;T)$ in the region of very small time. Checking the predictability requires determination of all q-dependent terms in the theory [see Eq. (5) for details], but previous work on it is fragmentary.

The present paper reports our approach to these prob-

lems by the time-resolved small-angle neutron scattering (SANS) method applied to a critical blend of normal (protonated) and deuterated polybutadienes. This method has a definite advantage over the LS method, since it permits us to investigate the scattering behavior in a wide region of q above the upper bound of the LS method.[18,19] Thus as shown below, it has become possible for the first time to see the structure factor $S(q,t;T)$ at such high q and to determine $q_m(t;T)$ and $S_m(t;T)$ in the very early stage of SD, where $S_m(t;T)$ is the scattering intensity at the peak of $S(q,t;T)$. The blend chosen is convenient for SANS measurement because it undergoes very slow SD, the typical characteristic time t_c[11] of which was of the order of 1000 s.[20] The deep quench was employed so that the scattering peak may become observable in the time scale accessible to our SANS facilities.

In conjunction with Problem 1, it remains to be clarified how much and how long the effect of the initial thermal concentration fluctuations in the system affects the subsequent SD. This effect is hereafter called *memory effect*. From a study on the SD kinetics of a binary blend of polystyrene (HPS)/poly(vinylmethylether) (PVME) by time-resolved LS, Okada and Han[21] concluded that the linearized theory of CHC,[17] which *includes the thermal fluctuation term*, can describe the early stage of SD in the shallow quench region. However, for deeper quench they found the time evolution of the structure factor to fit the usual Cahn–Hilliard equation which omits the thermal fluctuation term. They did not investigate a higher q range so that the question of whether the memory effect become pronounced or not in such a q range in the case of deep quench has been left unanswered. Mathematically the memory effect may be attributed to the inhomogeneous term (resulted from the thermal noise) in the inhomogeneous linear differential equation for the time-dependent concentration fluctuation.

In this series of papers, we focus on discussing (i) the effect of initial thermal fluctuation on SD kinetics and (ii) the applicability of the CHC linearized theory to our observed results.

II. EXPERIMENTAL SECTION

A. Samples

Both perdeuterated polybutadiene (DPB) and protonated polybutadiene (HPB) used in the present study were synthesized by living anionic polymerization. Table I summarizes their molecular characteristics. The two polymers are almost similar with respect to density and statistical segment length. As shown later (in Sec. III A), this blend has a nearly symmetric phase diagram. The glass transition temperature (T_g) of an HPB having similar microstructure is about -100 °C,[22] so that in the temperature range of SANS experiments reported here both DPB and HPB and also the blend are far above their corresponding T_g and hence behave like liquid in the long time limit.

DPB/HPB blend samples for time-resolved SANS experiments had a composition of 46.6 vol % DPB and 53.4 vol % HPB. A small amount of *N*-phenyl-2-naphthylamine (0.5 wt% of the total polymer weight) was added as an antioxidant. The composition chosen was a critical volume fraction predicted by the Flory–Huggins lattice theory.[23] Before SANS measurements each sample was dissolved in cyclohexane (approximately 7 wt% total polymer concentration) and then lyophilized. Our DPB/HPB blend was found to have an upper critical solution temperature (UCST) type phase diagram with a critical temperature at 99.2 °C from an analysis of SANS data in the single-phase state (see Sec. III A for details).[24] Thus if the mixture was stored at room temperature, it would undergo phase separation. For this reason, the mixture shortly after lyophilization was homogenized by mechanical mixing[25] at about 90 °C and then modeled into the spacer ring (1 mm in thickness and 14 mm in diameter) that would be used for scattering experiments. The samples were sandwiched between two quartz plates and put in a brass SANS cell. They were then brought to a temperature T_i at which they were in the single-phase state. The homogenization by mechanical mixing accelerates the rate at which the systems reaches thermal equilibrium at T_i.

TABLE I. Polymer characteristics.

Sample code	$M_n \times 10^{-4}$[a]	Z_w/Z_n[b]	Z_n[c]	Microstructure,[d] % 1,2	*cis*-1,4	*trans*-1,4
DPB	37.4	1.28	6223	21.5	36.3	42.2
HPB	27.3	1.06	5039	29.3	70.7[e]	

[a]Determined by membrane osmometry.
[b]Determined by size exclusion chromatography equipped with light scattering.
[c]Number-average degree of polymerization.
[d]Determined by $^{13}C-NMR$.
[e]Sum of *cis*-1,4 and *trans*-1,4.

B. Time-resolved SANS experiments

SANS data were taken by using the 30 m SANS instrument at the NIST Cold Neutron Research Facility and the pinhole collimation with a 10 Å neutron wavelength. The wavelength resolution, $\Delta\lambda/\lambda$, was 0.21, where λ is the wavelength of the neutron beam and $\Delta\lambda$ is the full width at half maximum (FWHM).

A copper heating block was used to maintain the sample within ± 0.2 °C of the desired temperature during each measurement. For the measurements at temperatures below 23 °C, a bath with a circulating mixture of ethylene glycol and ethanol (50/50 vol %/vol %) was used. Temperature-drops (T-drop) were carried out by manually transferring the sample at T_i into a copper block controlled to the measuring temperature T_f. In the present study three different temperatures 102.3 °C, 123.9 °C, and 171.6 °C were chosen for T_i and a single temperature -7.5 °C for T_f. It took about 4 to 5 min for the sample to settle down to T_f after the T-drop.

A time-resolved SANS profile at a given t was determined by counting over a time period of 3 min. A two-dimensional detector with a sample-to-detector distance of 15.30 m was used. The observed scattering intensity was

corrected accordingly for electronic background, sample transmittance and thickness, empty sample cell scattering, and detector inhomogeneity. The intensity was then converted to absolute units with a deuterated polystyrene (DPS) and HPS blend (50/50 wt%), which had been calibrated using a silica gel secondary standard[26] on the NIST 8 m SANS.[27] The corrected scattered intensity was circularly averaged to obtain the dependence of scattering intensity on the wave vector q [defined by $(4\pi/\lambda)\sin(\theta/2)$, with θ being the scattering angle].

III. RESULTS

A. Phase diagram

DPB/HPB blends with nine different compositions were prepared exactly in the same way as that described above and subjected to static SANS measurements to determine the phase diagram. The 8 m SANS instrument at the NIST Cold Neutron Research Facility[27] with a 9 Å neutron wavelength and a $\Delta\lambda/\lambda=0.25$ was used for these blends in the single-phase region.

Data for the static SANS structure factor, $S_T(q;T)$ were analyzed to evaluate the Flory–Huggins binary interaction parameter, $\chi(\phi,T)$, between DPB and HPB as a function of the volume fraction, ϕ, of DPB in the blend as well as T. To this end, the modified version[28,29] of the theory of de Gennes[30] for a single-phase binary polymeric blend was applied. Note that it assumes the mean-field model and the random-phase approximation (RPA). The details of the experimental method and data analysis will be reported elsewhere.[24]

We found that $\chi(\phi,T)$ at any given composition ϕ varied linearly with inverse absolute temperature (T^{-1}), consistent with many previous reports[29,31–33] and also that $\chi(\phi,T)$ at a given T was either almost independent of ϕ or very weakly dependent on ϕ over the range of ϕ from 0.182 to 0.781. A linear ϕ dependence of $\chi(\phi,T)$had been reported by Han *et al.*[34] for their DPS/PVME blends. The linear dependence of $\chi(\phi,T)$ on ϕ observed with our blends is expressed by

$$\chi(\phi,T)=-4.47\times10^{-4}+5.24\times10^{-5}\phi + (0.288-0.0346\phi)/T. \quad (1)$$

We note that the coefficients for ϕ in this expression are much smaller than those for the DPS/PVME blends. For the DPB/HPB blend with $\phi=0.466$ chosen for the kinetic experiments, χ as a function of T [hereafter noted $\chi(T)$] is given by

$$\chi(T)=-5.34\times10^{-4}+0.314/T. \quad (2)$$

The value of χ, χ_s, at the spinodal temperature T_s that was found to be 99.2 °C at the critical composition, was 3.10×10^{-4} when calculated by the method described in Ref. 31. Bates *et al.*[35] and Schwahn *et al.*[36] have reported a parabolic ϕ dependence of $\chi(\phi,T)$ for the isotopic mixture of poly(vinyl ethylene) and that of polystyrene, respectively.

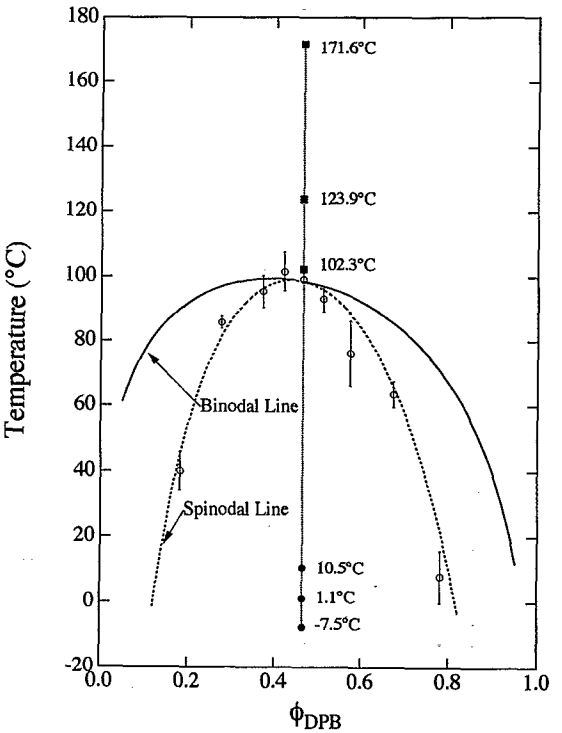

FIG. 1. Phase diagram of binary of DPB/HPB mixture. The solid and dashed lines correspond, respectively, to the binodal and spinodal calculated as described in the text. Unfilled circles are the experimentally determined spinodal temperatures at different compositions. Specimens were held at temperatures, T_i, shown by filled squares and then quenched to the destination temperatures, T_f, shown by filled circles.

Although Bates *et al.*[35] and Schwahn *et al.*[36] are studying different blend systems, however their conclusion does not accord with ours from the present work.

Figure 1 shows the phase diagram of our DPB/HPB system. The solid and dashed lines are, respectively, the binodal and spinodal lines calculated according to the Flory–Huggins theory with Eq. (1) for $\chi(\phi,T)$. We see that our DPB/HPB system has an UCST type phase diagram. The unfilled circles with error bars locate the spinodal temperatures estimated from intercepts between $\chi(\phi,T)$ at a given ϕ on the $\chi(\phi,T)$ vs $1/T$ (in K) plot and the lines $\chi=\chi_s(\phi)$. The filled squares and filled circles indicate T_i and T_f, respectively. The data taken at T_f other than −7.5 °C, i.e., 1.1 °C and 10.5 °C, will be reported in the subsequent paper.[20]

The quenching to −7.5 °C corresponds to a relatively deep quench, for which $\varepsilon[=(\chi(T_f)-\chi_s)/\chi_s]$ is 1.18.

B. General features of time-resolved SANS data

Figure 2 shows the time evolution of SANS profiles for our critical DPB/HPB mixture after the T-drop from 123.9 °C to −7.5 °C. Here the time-dependent structure factor, $S(q,t;T_f)$, is plotted against wave number q. The solid line in the lower part (a) of the figure shows the profile in the single phase at 123.9 °C. Similar data were obtained by T-drops from 102.3 °C to −7.5 °C and from 171.6 °C to −7.5 °C, but not shown here.

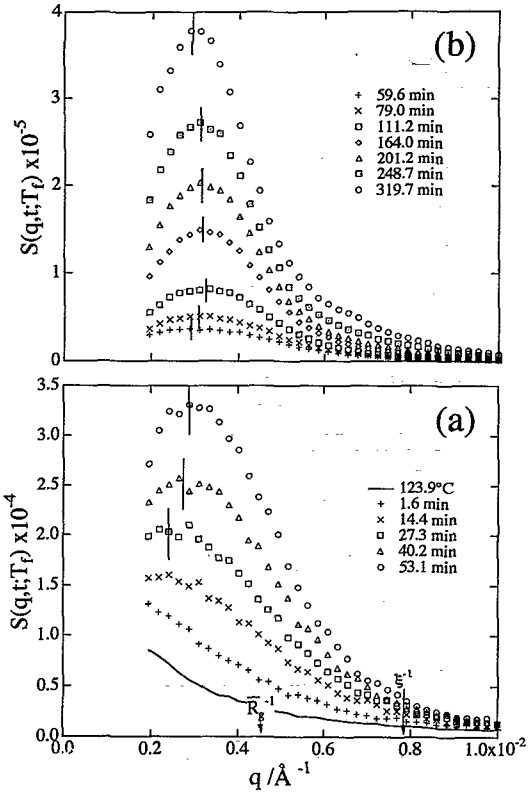

FIG. 2. Time evolution of SANS profiles for the critical DPB/HPB mixture after the T-drop from 123.9 °C (in the single phase state) to −7.5 °C (inside the spinodal phase boundary). (a) The early stage SD; (b) the intermediate stage SD. Vertical bars display the peak positions at different time. The wave numbers corresponding to $q=1/R_g$ and $q=1/\xi$ are shown by arrows.

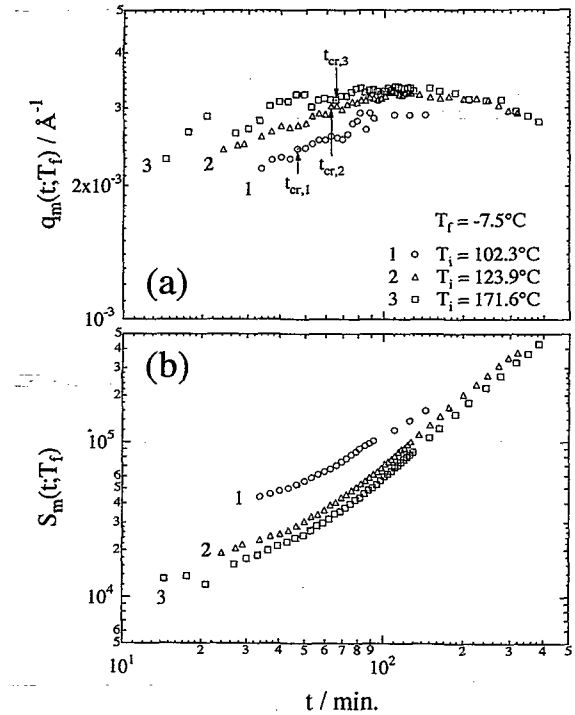

FIG. 3. Time changes in peak position $q_m(t;T_f)$ (part a) and peak intensity $S_m(t;T_f)$ (part b) for three different T_i as given in the figure. The crossover time $t_{cr,i}$ from the early to intermediate stage for each experiment is shown by an arrow.

As seen in Fig. 2(a), profiles start to show a maximum shortly after the quenching, and the maximum height $S_m(t;T_f)$ increases with t. In what follows, the q value at the maximum is denoted by $q_m(t;T_f)$. Surprisingly, $q_m(t;T_f)$ shifts to *larger values* at first (see the vertical segments of lines marked on the profiles from 27.3 to 111.2 min), stays constant for a while [see the profiles from 111.2 to 248.7 min and the constant value is defined as $q_m^M(T_f)$ hereafter] and eventually decreases with t (see the profiles after 248.7 min). This time dependence of $q_m(t;T_f)$ is significant even after considering the error ($\pm 3\times 10^{-4}$ Å^{-1} at most) associated with the determination of the peak position. The initial increase in $q_m(t;T_f)$ seems to contradict the results from computer simulations of the CHC linearized theory by Strobl *et al.*,[37] who showed that $q_m(t;T_f)$ either stayed unchanged or became smaller depending upon the parameters. Experimentally, Motowoka *et al.*[38] and Schwahn *et al.*[39] found this "initial peak-shift" to smaller q with t for their deuterated polycarbonate/PMMA and DPS/PVME blends, respectively. The mechanism of the unusual shift of $q_m(t;T_f)$ in the *very early stage of SD* is discussed below.

The wave number satisfying $q=1/\bar{R}_g$ is shown by an arrow in Fig. 2, where $\bar{R}_g$ is the mean radius of gyration for the DPB/HPB mixture defined below. Our deep quench experiments gave $q_m^M(T_f)$ that comes relatively close to $1/\bar{R}_g$, but $q_m^M(T_f)$ is *not* always equal to $q_m(0;T_f)$ because of the contribution of the thermal noise to $S(q,t;T_f)$. The true $q_m(0;T_f)$ is the wave number at which the growth rate of concentration fluctuations, $R(q;T)$, reaches a maximum.

The thermal correlation length ξ for thermal concentration fluctuations is another important parameter, the definition of which will be presented in Sec. IV A. ξ at −7.5 °C was calculated to be 127.4 Å. The wave number satisfying $q=\xi^{-1}$ is shown in Fig. 2 by another arrow.

Figure 3 shows plots of $q_m(t;T_f)$ and $S_m(q;T_f)$ vs t. We see more clearly the initial peak shift of the peak toward larger q and the increase in intensity with t. Summarizing, as time goes on, $q_m(t;T_f)$ increases, stays unchanged, and then decreases, while $S_m(t;T_f)$ keeps increasing. The other important observation is that, depending upon T_i at which the specimen is held prior to a T-drop, $q_m(t;T_f)$ and $S_m(t;T_f)$ follow different time dependencies. Remarkably, this memory effect persists for a considerably long period of time in the subsequent SD process; in fact, it eventually disappeared (at about 300 min after the onset of SD). It is also observed that the higher the T_i, hence the smaller the thermal concentration fluctuations before the T-drop, the sooner $q_m(t;T_f)$ reaches a constant value and the smaller the shift of $q_m(t;T_f)$ in the very early stage becomes.

Figure 4 demonstrates how the $S(q,t;T_f)$ at representative times depend on T_i. The profiles show considerable dissimilarity, especially in scattering intensity. Thus $S(q,t;T_f)$ for $T_i=102.3$ °C is the largest; $S(q,t;T_f)$ for

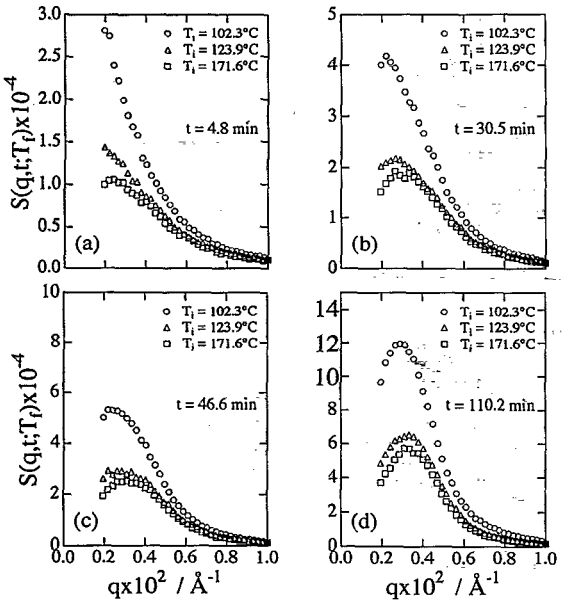

FIG. 4. Comparison of the SANS scattering profiles after the T-drop from three different T_i (as indicated) to T_f (=−7.5 °C) at (a) t=4.8, (b) t=30.5, (c) t=46.6, and (d) t=110.2 min.

T_i=171.6 °C is the smallest; $S(q,t;T_f)$ for T_i=123.9 °C is intermediate. This order was maintained over a wide span of time up to about 300 min, and became parallel with the order of the scattering functions $S_T(q;T=T_i)$ prior to the T-drop. It is rather surprising to see that thermal concentration fluctuations present at $T=T_i$ affect the time evolution of $S(q,t;T_f)$ for as long a time as 300 min after the onset of SD.

IV. ANALYSIS AND DISCUSSION

A. Theoretical background (Cahn–Hilliard–Cook theory)

The time evolution of the structure factor, $S(q,t)$, for a binary mixture undergoing spinodal decomposition is generally described by the following nonlinear differential equation[3,6] if the hydrodynamic effects[4] may be neglected

$$\frac{\partial S(q,t)}{\partial t}=-2\frac{\Lambda(q)q^2}{k_BT}\left\{\left[\left(\frac{\partial^2 f}{\partial\phi^2}\right)_{\phi=\phi_0}+2\kappa q^2\right]S(q,t)+\frac{1}{2}\left(\frac{\partial^3 f}{\partial\phi^3}\right)_{\phi=\phi_0}S_3(q,t)+\frac{1}{6}\left(\frac{\partial^4 f}{\partial\phi^4}\right)_{\phi=\phi_0}S_4(q,t)+\cdots\right\}+2\Lambda(q)q^2. \quad (3)$$

Here $\Lambda(q)$ is the q-dependent Onsager kinetic coefficient,[40,41] f the free energy density for the uniform mixture at a phase separation temperature T, ϕ_0 the initial composition, κ an interfacial free energy coefficient defined as the proportionality constant in the relation between the interfacial free energy density and the square of concentration gradient, and k_B the Boltzmann constant. The last term in Eq. (3) arises from the thermal noise.[17] $S_n(q,t)$ is defined by

$$S_n(q,t)=\int d\mathbf{r}\langle[\phi(\mathbf{r},t)-\phi_0]^{n-1}[\phi(0,t)-\phi_0]\rangle e^{i\mathbf{q}\mathbf{r}}, \quad (4)$$

where $\phi(\mathbf{r},t)$ is the local concentration of one component at position $\mathbf{r}$ and time t and the angular brackets denote the thermal average. Approximate solutions to Eq. (3) have been proposed by Langer, Bar-on, and Miller.[6]

In the early stage SD, the concentration fluctuations are so small that higher order terms, $S_n(q,t)$, may be neglected. Then, Eq. (3) is reduced to an inhomogeneous linear differential equation for $S(q,t)$, and its solution reads[17]

$$S(q,t;T_f)=S_T(q;T_f)+[S(q,0;T_f)-S_T(q;T_f)]\exp[2R(q;T_f)t], \quad (5)$$

where

$$S_T(q;T_f)=-\frac{\Lambda(q;T_f)q^2}{R(q;T_f)}. \quad (6)$$

Here $S_T(q;T_f)$ is the structure factor $S_T(q;T)$ at $T=T_f$ and is called the virtual structure factor.[40] $S(q,0;T_f)$ is the structure factor at the onset of SD at $T=T_f$, and $R(q;T_f)$ is the growth rate of the concentration fluctuation corresponding to the wave number q. It is worth noting that all terms in Eq. (5) refer to T_f only but, as will be seen, they depend on the structure factor at the "initial" temperature T_i. We will return to this point in Sec. IV B.

Since the system at $T=T_f$ cannot stay in one-phase, $S_T(q;T_f)$ is not directly measurable and hence is called "virtual" structure factor. It has to be inferred. One method is experimental. It uses an extrapolation of $S_T(q;T)$ measured at a series of T in the single-phase region to $T=T_f$. The other is theoretical. It invokes a theory for $S_T(q;T)$. Here we used the latter, taking as an adequate approximation the extended version[28] of de Gennes' theory for a binary polymer mixture consisting of the components each having a Schultz–Zimm molecular weight distribution and different monomer molecular volume. It reads[29]

$$S_T(q;T)=\left[\frac{\nu_0}{\phi_A\langle Z_A\rangle_n\nu_A S_A(q)}+\frac{\nu_0}{\phi_B\langle Z_B\rangle_n\nu_B S_B(q)}-2\chi(T)\right]^{-1}, \quad (7)$$

where

$$S_i(q)=\frac{2}{X_i^2}\left[\left(\frac{h_i}{h_i+X_i}\right)^{h_i}-1+X_i\right] \quad (i=A \text{ or } B) \quad (8)$$

with

$$X_i=q^2\langle R_{gi}^2\rangle_n=q^2\langle z_i\rangle_n b_i^2/6 \quad (9a)$$

and

$$h_i=[(\langle z_i\rangle_w/\langle z_i\rangle_n)-1]^{-1} \quad (9b)$$

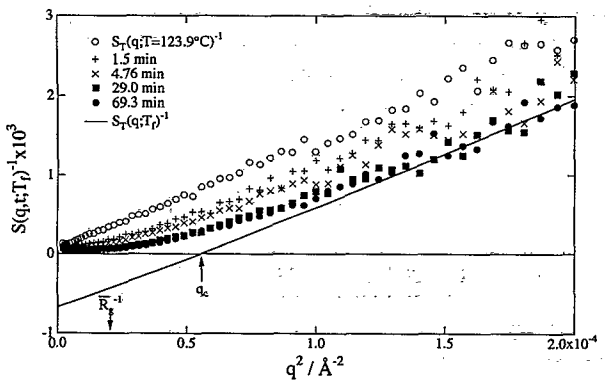

FIG. 5. Plot of inverse structure factor $S(q,t;T_f)^{-1}$ vs q^2 for the critical DPB/HPB mixture quenched from 123.9 °C to −7.5 °C. Solid line indicates inverse of the calculated virtual structure factor $S_T(q;T_f)^{-1}$ as a function of q^2.

$\langle z_i\rangle_w$ and $\langle z_i\rangle_n$ denote, respectively, the number- and weight-average degree of polymerization for the ith component ($i=A$ and B), and ϕ_i is the volume fraction of the ith component with molar volume v_i and statistical segment length b_i. v_0 is the molar volume of the reference cell defined as $v_0=(\phi_A/v_A+\phi_B/v_B)^{-1}$, and χ is Flory's segmental interaction parameter.

The value of $\chi(T_f)$ needed to calculate $S_T(q;T_f)$ from Eq. (7) was estimated by assuming that Eq. (2) is valid down to T_f. With $\chi(T_f)$ thus obtained, the correlation length ξ for thermal concentration fluctuations at $T=T_f$ can be calculated from

$$\xi^2=\frac{v_0}{36}\frac{1}{\chi(T_f)-\chi_S}\left[\frac{b_A^2}{v_A\phi_A}\frac{\langle Z_A\rangle_z}{\langle Z_A\rangle_w}+\frac{b_B^2}{v_B\phi_B}\frac{\langle Z_B\rangle_z}{\langle Z_B\rangle_w}\right], \tag{9c}$$

where $\langle Z_i\rangle_z$ denotes the z-averaged degree of polymerization of component i ($i=A$ and B).

B. Data analysis with the Cahn–Hilliard–Cook theory

Equation (5) representing the CHC theory contains three functions $S_T(q;T_f)$, $S(q,0;T_f)$, and $R(q;T_f)$. As mentioned in Sec. I, one of the main aims of our work was to determine their actual forms and look at their features. Conveniently we call this operation the CHC analysis.

We have already determined the first function $S_T(q;T_f)$ using the extended version of de Gennes' theory [Eq. (7)]. It becomes negative at q smaller than the critical wave number, $q_c=7.44\times10^{-3}$ Å^{-1}, as seen in Fig. 5. According to Eqs. (5) and (6), $S(q,t;T_f)$ in the region of q greater than q_c where $R(q;T_f)$ is negative should approach $S_T(q;T_f)$ as t increases. To confirm this prediction, in Fig. 5, we plot $S(q,t;T_f)^{-1}$ against q^2 for different values of t after the T-drop from 123.9 °C to −7.5 °C. It is seen that $S(q,t;T_f)^{-1}$ at any q monotonously decreases with increasing t and those for q larger than 1.2×10^{-2} Å^{-1} essentially converge to the solid line that represents $S_T(q;T_f)^{-1}$ plotted against q^2. Thus the data prove that $R(q;T_f)$ for q above a certain value is negative and that the structure factor $S_T(q;T_f)$ determined experimentally from

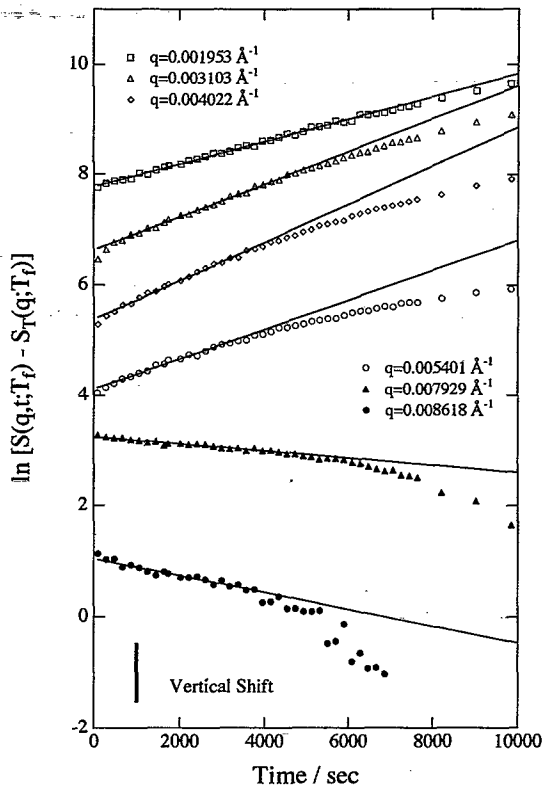

FIG. 6. Plot of $\ln[S(q,t;T_f)-S_T(q;T_f)]$ vs t at six different wave numbers for the critical DPB/HPB mixture quenched from 123.9 °C to −7.5 °C. Curves except that for $q=1.953\times10^{-3}$ Å^{-1} have been vertically shifted to avoid congestion. Vertical line at the lower left corner represents the amount of the relative shift.

$\lim_{t\to\infty} S(q,t;T_f)$ for q above this value is consistent with the calculated $S_T(q;T_f)$ based on Eq. (7). This supports the correctness of our choice of $S_T(q;T_f)$.

It is in order to note that the term $\Delta\equiv[S(q,0;T_f)-S_T(q;T_f)]$ in Eq. (5) is negative at $q>q_c$. Therefore, $\Delta\exp[2R(q;T_f)t]$ decreases in its absolute value with t, giving rise to an increase in $S(q,t;T_f)$ from $S(q,0;T_f)$ to the equilibrium value $S_T(q;T_f)$ [see Eq. (5)]. At $q<q_c$ $R(q;T_f)>0$ and $\Delta>0$, so that $S(q,t;T_f)$ increases with t. Thus, the concentration fluctuation or the structure factor $S(q,t;T_f)$ always increases with t over the whole range of q.

Once $S_T(q;T_f)$ was calculated, the remaining quantities to be evaluated in the CHC analysis are $R(q;T_f)$ and $S(q,0;T_f)$. Figure 6 illustrates how these can be determined. Here $\ln[S(q,t;T_f)-S_T(q;T_f)]$ at various q are plotted against t (in s) for the T-drop experiment from 123.9 °C to −7.5 °C. For clarity, the plots except that for $q=1.953\times10^{-3}$ Å^{-1} have been shifted vertically. The data points at any given q are seen to initially follow a straight line, indicating that there is a regime where Eq. (5) holds. Deviations from the linearity at a later time are believed to be due to the onset of the later stage SD (intermediate and late stage SD). The time at which the deviation starts depends on q; the higher the value q, the earlier the deviation takes place. The slope and intercept (at $t=0$) of each

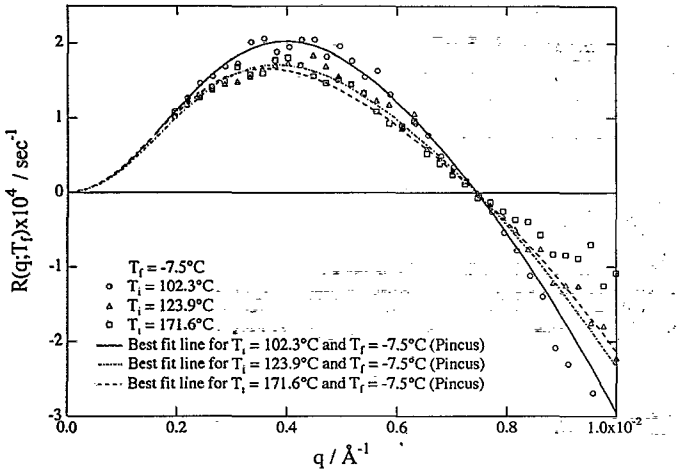

FIG. 7. Q dependence of $R(q;T_f)$ obtained from experiments with three different T_i=102.3 °C, 123.9 °C, and 171.6 °C and one T_f=−7.5 °C.

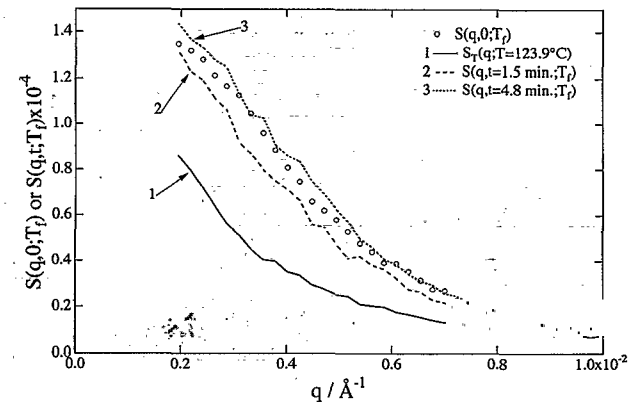

FIG. 8. Plot of the effective initial structure factor, $S(q,0;T_f)$ vs q for the critical DPB/HPB mixture encountered by T-drop from 123.9 to −7.5 °C together with $S_T(q;T=123.9\,°C)$ (curve 1) and the time-dependent SANS structure factor at $t=1.5$ (curve 2) and 4.8 min (curve 3).

straight line allows $R(q,T_f)$ and $S(q,0;T_f)$ to be evaluated.

Figure 7 shows the q dependence of $R(q;T_f)$ thus determined for T_i=102.3 °C, 123.9 °C, and 171.6 °C and T_f =−7.5 °C. The lines show the best fits to the Pincus theory,[41] achieved by the method which will be discussed in a companion paper.[20] No substantial differences can be seen among the data for different T_i within the accuracy of our measurements. This implies that thermal concentration fluctuations at $T=T_i$ have no essential effect on $R(q;T_f)$. In other words, $R(q;T_f)$ depends solely on the phase separation temperature T_f and hence not affected by the memory effect. We also see that, as q increases, $R(q;T_f)$ for different T_i turns to be negative at the same q value (7.74×10^{-3} Å^{-1}). This is identified to q_c at which $S_T(q;T_f)^{-1}$ vanishes (see Fig. 5). This behavior is what is predicted from Eq. (6) if $\Lambda(q;T_f)$ does not vanish at q_c. The q value for the maximum of $R(q;T_f)$ is what we have denoted by $q_m(0;T_f)$. Its values for different T_i are listed in Table II, along with $q_c/q_m(0;T_f)$. This ratio is about 2.0, differing from 1.4 ($2^{1/2}$) predicted from the Cahn–Hilliard (CH) theory that neglects the thermal noise effect. However, the disparity cannot be simply associated with thermal noise, but the q dependence of $\Lambda(q;T_f)$ is also responsible for it as seen from Eq. (6).

The "*effective initial structure factor*" $S(q,0;T_f)$ for the T-drop from T_i(=123.9 °C) to T_f(=−7.5 °C) is shown by unfilled circles in Fig. 8. The solid line (curve 1) representing $S_T(q;T=123.9\,°C)$ appears below $S(q,0;T_f)$. The same trend has been observed at other T_i, as shown in Fig. 9. If, in the T-drop from 123.9 to −7.5 °C, the temperature of the specimen had reached T_f instantaneously, $S(q,0;T_f)$ would have been very close to $S_T(q;T=123.9\,°C)$. Actually, it took a finite time to cool the specimen to T_f, so that the specimen passed the spinodal region at a finite rate and so should have undergone SD athermally until it reached T_f. This mechanism explains why $S(q,0;T_f)$ deviates significantly from $S_T(q;T=123.9\,°C)$. In Fig. 8, the structure functions at $t=1.5$ and 4.8 min are plotted against q by a dashed (curve 2) and a broken line (curve 3), respectively. Interestingly, $S(q,0;T_f)$ appears in between these two lines, indicating that the specimen settled down to T_f at a time somewhere between 1.5 and 4.8 min after the T-drop. Actually, this time was about 4 to 5 min.

Data for $S(q,0;T_f)$ from the experiments with three different T_i are displayed together with the corresponding $S_T(q;T=T_i)$ in Fig. 9. Again we see that $S(q,0;T_f)$ al-

TABLE II. Wave numbers, $q_m(0;T_f)$, at the maximum of $R(q;T_f)$ and the ratio of q_c to $q_m(0;T_f)$.

Initial temperature, T_i(°C)	$q_m(0;T_f)\times10^3$ (Å^{-1})[a]	$q_c/q_m(0;T_f)$[b]
102.3	3.90±0.05	1.91±0.04
123.9	3.79±0.04	1.97±0.04
171.6	3.71±0.05	2.01±0.04

[a] T_f=−7.5 °C for all experiments.
[b] q_c=(7.44±0.05)×10^{-3} Å^{-1} at T_f=−7.5 °C.

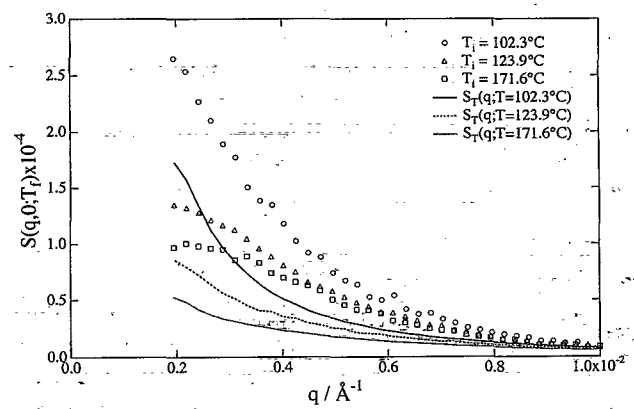

FIG. 9. Effective initial structure factor $S(q,0;T_f)$ for three different T_i=102.3 °C, 123.9 °C, and 171.6 °C (the profiles shown by data points) are plotted against q together with the corresponding $S_T(q;T=T_i)$ (the profiles shown by lines).

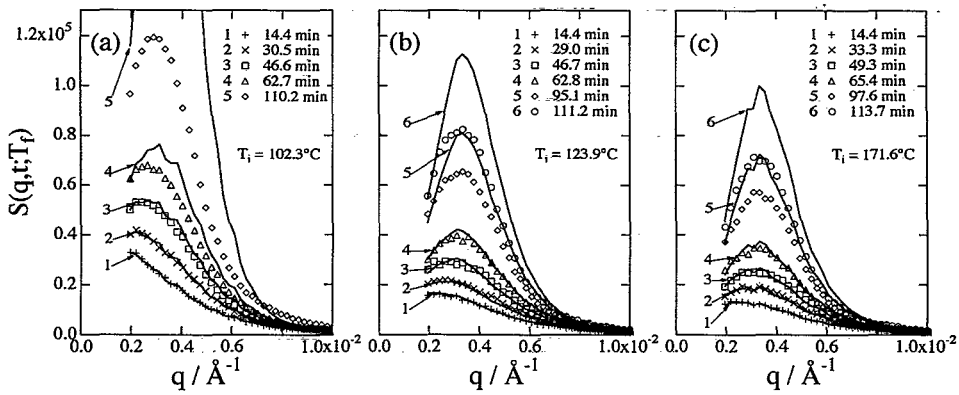

FIG. 10. $S(q,t;T_f)$ vs q for T_i=102.3 °C, 123.9 °C, and 171.6 °C (shown by various symbols) and the predicted $S(q,t;T_f)$ according to the CHC theory (solid lines).

ways appears above $S_T(q;T=T_i)$. Importantly, there is a parallelism between $S(q,0;T_f)$ and $S_T(q;T=T_i)$ with T_i: both are largest for T_i=102.3 °C, intermediate for T_i =123.9 °C, and smallest for T_i=171.6 °C. Thus the initial fluctuations at T_i crucially affect $S(q,0;T_f)$ in such a way that the larger the initial fluctuations, the higher the $S(q,0;T_f)$ becomes. Thus mathematically, $S(q,0;T_f)$ should be considered as a function of T_i as well as q and T_f.

We now proceed to consider why the peak of $S(q,t;T_f)$ shifts to higher q in the very beginning of the phase separation. Though it may look unreasonable at a glance, the behavior is not unexpected if we consider that $S(q,t;T_f)$ depends on three q-dependent functions $S_T(q;T_f)$, $S(q,0;T_f)$, and $R(q;T_f)$ through Eq. (5). To confirm this we calculated $S(q,t;T_f)$for a series of t by substituting the above obtained numerical data for three functions into Eq. (5). The solid lines in Figs. 10(a), 10(b), and 10(c) illustrate the results for the T-drops from T_i=102.3 °C, 123.9 °C, and 171.6 °C to T_f=−7.5 °C. It is seen that they reproduce the corresponding observed behavior up to, at least, 46.6, 62.8, and 65.4 min for Figs. 10(a), 10(b), and 10(c), respectively. These times may be identified as the times t_{cr} at which SD crosses over to the intermediate stage in the sense that Eq. (5) is for the early stage SD.[11] Remarkably the peaks of the calculated lines in Fig. 10 shift toward higher q as t increases in the early stage of SD, just as the experimental data show. Thus, we can conclude that the CHC theory expressed by Eq. (5) is well consistent with our experimental findings on the early stage SD.

The above-mentioned t_{cr} values are indicated by arrows in Fig. 3 where $t_{cr,i}$ (i=1 to 3) denote the t_{cr} for T_i=102.3, 123.9, and 171.9 °C, respectively. Looking at the arrows one notices that the time domain where $q_m(t;T_f)$ is independent of t belongs to the intermediate stage SD rather than the early stage SD. This problem will be considered again in our forthcoming paper.[20] The increase in $q_m(t;T_f)$ in the early stage SD for a given T_i is due to the thermal noise put in the sample as a memory. The appearance of the time-independent $q_m(t;T_f)$ is a result of the cancellation of the above effect by the nonlinear effect which tends to decrease $q_m(t;T_f)$.

In Fig. 11(a), where the data are reproduced from Fig. 10(b), the solid lines have been constructed in the same way as above but with $S_T(q;T=123.9\,°C)$ taken as $S(q,0;T_f)$. None of them are seen to fit correctly the plotted experimental points; the calculated profiles are consistently lower than the observed. Finally, we note that the zig–zag nature of the calculated profiles in Figs. 10 and 11 reflects those of observed $S(q,0;T_f)$ and $S_T(q;T=123.9\,°C)$ that have been put in the numerical computations.

We have demonstrated that the CHC theory can reproduce the observed peak shift toward larger q in the very early time of SD. This initial peak shift, however, can be understood from a qualitative considerations as follows. The T-drop, from T_i to T_f, takes a finite time, so that concentration fluctuations in the specimen begin to grow before reaching T_f after crossing the phase boundary. Owing to this effect, the excess scattering having different q dependence adds up to $S_T(q;T=T_i)$ and makes the initial

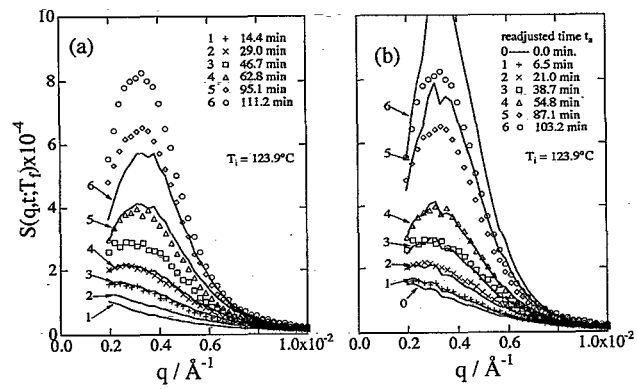

FIG. 11. $S(q,t;T_f)$ vs q after the T-drop from 123.9 °C to −7.5 °C (shown by various symbols) and the predicted $S(q,t;T_f)$ according to the CHC theory (solid lines). (a), $S(q,t;T_f)$ calculated by assuming $S(q,0;T_f)$ $=S_T(q;T=123.9\,°C)$. (b), $S(q,t;T_f)$ calculated by assuming $S(q,0;T_f)=S(q,t_a=0;T_f)$ where t_a is a new time scale defined in the text.

structure function $S(q,0;T_f)$ different from $S_T(q;T=T_i)$. Thus $S(q,0;T_f)$ should have a memory which consists of the concentration fluctuation at $T=T_i$ and the path of the temperature drop. If the change in temperature of the specimen during the T-drop were precisely measured, it would be possible to quantify the memory on the basis of the CHC theory.

If one neglects $S_n(q,t)$, Eq. (3) becomes linear as mentioned in Sec. IV A. What is important is that this linearized version of Eq. (3) is *inhomogeneous* because of the last term (thermal noise term) on its right-hand side. Therefore, the solution to it depends on initial thermal concentration fluctuations, and this fact makes it important to define the initial condition precisely. In calculating the lines in Fig. 10, we used $S(q,0;T_f)$ derived from the CHC analysis for this condition. It is important that this $S(q,0;T_f)$ is not the same as $S_T(q;T=T_i)$ for the reason mentioned in the previous paragraph.

C. Alternative data analysis with Cahn–Hilliard–Cook theory

Since it took about 4 to 5 min for the specimen to cool to T_f in all of our experiments, it seems reasonable to redefine $S(q,0;T_f)$. For example, we may identify $S(q,t;T_f)$ at the third scan taken about 6 to 9 min after the T-drop to be the $S(q,t_a=0;T_f)$, i.e., $I(q,t=t_3;T_f)=I(q,t_a=0;T_f)$, where t_a is a new time defined by

$$t_a=t-t_3, \tag{10}$$

with t_3 being the time at the third scan. We confirmed that at the beginning of the third scan the temperature of the specimen had already settled down to $T=T_f$. This alternative approach has an advantage such that the initial state can be well defined. It requires one to adjust the starting time for the SD process from 0 to t_a. Similar idea has been used in the reverse quench case.[42] In Fig. 11(b), we compare measured $S(q,t_a;T_f)$ with the structure factor constructed in the same way as above but with t replaced by $t-7.98$ (min) and $S(q,t_a=0;T_f)$ equated to $S(q,0;T_f)$. It is clearly seen that the calculated lines can predict $S(q,t_a;T_f)$ data well and the peak shift in the very early time of SD. Thus we conclude that once $S(q,0;T_f)$ in the CHC theory is accurately determined, the theory can describe the time change in the scattering profile even when the quenching from T_i to T_f cannot be carried out ideally rapidly.

V. CONCLUSIONS

This paper has dealt with the self-assembling process at the critical composition of a mixture of DPB and HPB that has an UCST type phase diagram. The spinodal temperature of this mixture was 99.2 °C. Phase separation via SD was induced by quenching the system from T_i (in the single-phase region) to T_f (in the spinodal region). In order to see the effect of thermal concentration fluctuations existing at $T=T_i$, three different T_i (102.3 °C, 123.9 °C, and 171.6 °C) were chosen while T_f was fixed at -7.5 °C. The time evolution of the structure factor after quenching was followed using the time-resolved small-angle neutron (SANS) scattering method.

Experimentally obtained time-dependent SANS structure factor, $S(q,t;T_f)$, clearly showed maxima expected in the early stage SD (Fig. 2). It was found that (i) depending upon T_i at which the system was held in the single-phase, $q_m(t;T_f)$ as well as $S_m(t;T_f)$ followed different time changes in the beginning of phase separation (Fig. 3); (ii) comparison of $S(q,t;T_f)$ at a given t for different T_i made it clear that the lower the T_i (and hence the larger the SANS structure factor in the single-phase state before quenching), the more the $S(q,t;T_f)$ is enhanced up to about 300 min [Figs. 3(b) and 4]. Thus we concluded that the thermal concentration fluctuations present in the system before quenching *do* affect both the early stage SD and the early phase of the intermediate stage SD and hence the coarsening process.

Comparison between experimentally observed $S(q,t;T_f)$ and the linearized theory of Cahn, Hilliard, and Cook (CHC) led to the finding that the growth rate $R(q;T_f)$ of concentration fluctuations is essentially independent of T_i and that there is a wave number q_c such that $R(q;T_f)$ is positive at $q<q_c$, zero at $q=q_c$, and negative at $q>q_c$ (see Fig. 7). The effective initial structure factor at $T=T_f$, $S(q,0;T_f)$, was always larger than $S_T(q;T=T_i)$. This behavior was interpreted in terms of the athermal SD occurring during the T-drop that can be attributed to a finite time needed for a T-drop. We found a correlation between $S(q,0;T_f)$ and T_i: the higher the T_i, the smaller the $S(q,0;T_f)$ is. This experimental finding evidences that thermal concentration fluctuations in the single-phase state before T-drop contribute to $S(q,0;T_f)$.

The time evolution of $S(q,t;T_f)$ which was reconstructed by use of the CHC theory successfully describes the observed features of the early stage SD process, including the initial peak shift toward larger q (see Figs. 10 and 11).

ACKNOWLEDGMENTS

The authors gratefully appreciate the help received from Dr. C. J. Glinka and Dr. John Barker at the National Institute of Standards and Technology with SANS measurements. The authors also thank Nippon Zeon Co. for providing HPB sample used in this study.

[1] T. Hashimoto, Phase Transitions **12**, 47 (1988); T. Hashimoto, in *Materials Science and Technology*, edited by R. W. Cahn, P. Haasen, and E. J. Kramer (VCH, Weinheim, 1993, in press) Vol. 12, Chap. 6.
[2] T. Nose, Phase Transitions **8**, 245 (1987).
[3] J. D. Gunton, M. San Miguel, and P. S. Sahni, *Phase Transition and Critical Phenomena*, edited by C. Domb and J. L. Lebowitz (Academic, New York, 1983), Vol. 8, p. 269.
[4] K. Kawasaki, Prog. Theor. Phys. **57**, 826 (1977); K. Kawasaki and T. Ohta, *ibid.* **59**, 362 (1978).
[5] K. Binder, in *Materials Science and Technology*, edited by R. W. Cahn, P. Haasen, and E. J. Kramer (VCH, Weinheim, 1990), Vol. 5, Chap. 7.
[6] J. S. Langer, M. Bar-on, and H. D. Miller, Phys. Rev. A **11**, 1417 (1974).
[7] A. Chakrabarti, A. Toral, J. D. Gunton, and M. Muthukumar, Phys. Rev. Lett. **63**, 2072 (1989); A. Chakrabarti, A. Toral, J. D. Gunton, and M. Muthukumar, J. Chem. Phys. **92**, 6899 (1990).

[8] T. Koga and K. Kawasaki, Phys. Rev. A **44**, R817 (1991).
[9] Y. Oono and S. Puri, Phys. Rev. A **38**, 434 (1988); A. Shinozaki and Y. Oono, Phys. Rev. Lett. **66**, 173 (1991).
[10] H. L. Snyder and P. Meakin, J. Chem. Phys. **79**, 5588 (1983).
[11] T. Hashimoto, M. Itakura, and N. Shimizu, J. Chem. Phys. **85**, 6773 (1986).
[12] F. S. Bates and P. Wiltzius, J. Chem. Phys. **91**, 3258 (1989).
[13] T. Kyu and M. Saldanha, Macromolecules **21**, 1021 (1988).
[14] J. W. Cahn, Acta Metall. **9**, 795 (1961); J. Chem. Phys. **42**, 93 (1965).
[15] H. Jinnai, H. Hasegawa, T. Hashimoto, and C. C. Han, Macromolecules **24**, 282 (1991).
[16] T. Hashimoto, M. Takenaka, and H. Jinnai, J. Appl. Cryst. **24**, 457 (1991); M. Takenaka, T. Izumitani, and T. Hashimoto, J. Chem. Phys. **92**, 4566 (1990); M. Takenaka and T. Hashimoto, *ibid.* **96**, 6177 (1992).
[17] H. E. Cook, Acta Metall. **18**, 287 (1970).
[18] J. S. Higgins, H. Fruitwala, and P. E. Tomlins, Macromolecules **22**, 3674 (1989); J. S. Higgins, H. Fruitwala, and P. E. Tomlins, Br. Polym. J. **21**, 247 (1989).
[19] W. Pyckhout, D. Schwahn, I. Sosnowska, T. Springer, and H. Yee-Madeira, Physica B **156–157**, 402 (1989).
[20] H. Jinnai, H. Hasegawa, T. Hashimoto, and C. C. Han, J. Chem. Phys. (to be published).
[21] M. Okada and C. C. Han, J. Chem. Phys. **85**, 5317 (1986).
[22] H. L. Stephens, *Polymer Handbook,* 3rd ed., edited by J. Brandup and E. H. Immergut (Wiley, New York, 1989), p. V-1.
[23] P. J. Flory, J. Chem. Phys. **9**, 660 (1941); M. L. Huggins, *ibid.* **9**, 440 (1941).
[24] H. Jinnai, H. Hasegawa, T. Hashimoto, and C. C. Han, Macromolecules (to be submitted).
[25] T. Hashimoto, T. Izumitani, and M. Takenaka, Macromolecules **22**, 2293 (1989).
[26] C. J. Glinka and S. Krueger, NBS Memorandum for SANS Users, Dec. 29, 1986.
[27] C. J. Glinka, J. M. Rowe, and J. G. LaRock, J. Appl. Cryst. **19**, 427 (1986).
[28] M. Warner, J. S. Higgins, and A. J. Carter, Macromolecules **16**, 1931 (1983); M. Shibayama, H. Yang, R. S. Stein, C. C. Han, *ibid.* **18**, 2179 (1985).
[29] S. Sakurai, H. Hasegawa, T. Hashimoto, I. Glen Hargis, S. L. Aggarwal, and C. C. Han, Macromolecules **23**, 451 (1990).
[30] P. G. de Gennes, *Scaling Concepts in Polymer Physics* (Cornell University, Ithaca, NY, 1979).
[31] H. Jinnai, H. Hasegawa, T. Hashimoto, and C. C. Han, Macromolecules **25**, 6078 (1992).
[32] F. S. Bates, S. B. Dierker, and G. D. Wignall, Macromolecules **19**, 1938 (1986).
[33] N. P. Balsara, L. J. Fetters, N. Hadjichristidis, D. J. Lohse, C. C. Han, W. W. Graessley, and R. Krishnamoorti, Macromolecules **25**, 6137 (1992).
[34] C. C. Han, B. J. Bauer, J. C. Clark, Y. Muroga, Y. Matsushita, M. Okada, Q. Tran-Cong, T. Chang, and I. C. Sanchez, Polymer **29**, 2002 (1988).
[35] F. S. Bates, M. Muthukumar, G. D. Wignal, and L. J. Fetters, J. Chem. Phys. **89**, 535 (1988).
[36] D. Schwahn, K. Hahn, and T. Springer, J. Chem. Phys. **93**, 8383 (1990).
[37] G. R. Strobl, Macromolecules **18**, 558 (1985).
[38] M. Motowoka, H. Jinnai, T. Hashimoto, Y. Qiu, and C. C. Han, J. Chem. Phys. **99**, 2095 (1993).
[39] D. Schwahn, S. Janssen, and T. Springer, J. Chem. Phys. **97**, 8775 (1992).
[40] K. Binder, J. Chem. Phys. **79**, 6387 (1983).
[41] P. Pincus, J. Chem. Phys. **75**, 1996 (1981).
[42] A. Z. Akcasu, I. Bahar, B. Erman, Y. Feng, and C. C. Han, J. Chem. Phys. **97**, 5872 (1992).